inorganics

MDPI

Article

Supramolecular Aggregation of a New Substituted Bis(salicylaldiminato)zinc(II) Schiff-Base Complex Derived from *trans*-1,2-Diaminocyclohexane

Giuseppe Consiglio *, Ivan Pietro Oliveri, Salvatore Failla and Santo Di Bella *

Dipartimento di Scienze Chimiche, Università di Catania, I-95125 Catania, Italy; ivan.oliveri@alice.it (I.P.O.); sfailla@dii.unict.it (S.F.)

* Correspondence: gconsiglio@dii.unict.it (G.C.); sdibella@unict.it (S.D.B.); Tel.: +39-095-738-5068 (G.C. & S.D.B.)

Received: 1 December 2017; Accepted: 29 December 2017; Published: 1 January 2018

Abstract: In this contribution is reported the synthesis, characterization, and aggregation properties in solution of a novel Zn(II) complex, (***R***)-**2**, derived from the enantiopure chiral *trans*-1,2-diaminocyclohexane and a substituted salicylaldehyde. Detailed ^{1}H NMR, DOSY NMR, optical absorption, and circular dichroism spectroscopic studies and chemical evidence allowed to investigate the nature of aggregate species in solution. The high solubility of (***R***)-**2** in solution of the non-coordinating chloroform solvent leads to formation of various aggregates, some of them consisting of large oligomers estimated to contain up to 27 monomeric units. The chiral *trans*-stereochemistry of the bridging diamine favors a different aggregation mode in these complexes, both in the oligomers and dimers, involving a tetrahedral coordination geometry around the metal center. Overall data suggest the formation of helical oligomers, $(ZnL)_n$, in freshly prepared chloroform solutions which, by standing or heating, evolve towards a more thermodynamically stable, dinuclear double-helicate Zn_2L_2 dimer.

Keywords: zinc(II) complexes; Schiff-bases; molecular aggregation; chiral oligomers

1. Introduction

Molecular aggregation is a topic of current interest involving various properties and applications [1–4]. In recent years we have been involved in the study of the aggregation properties of bis(salicylaldiminato)zinc(II) Schiff-base complexes, derivatives from substituted salicylaldehydes and 1,2-diamines [5–11]. Their aggregation properties are related to the Lewis acidic character of the metal center which, in turn, is strongly connected to the nature of the bridging diamine [12]. Therefore, a variety of supramolecular architectures [13–18], mesomorphic [19–22], and self-assembled nanostructures [23–27] have been found, mostly because of intermolecular Zn···O axial interactions involving pentacoordinated square-pyramidal Zn(II) geometries. Moreover, these species exhibit interesting photophysical properties [28–31] and are sensors of various Lewis bases [32–53].

In this context, a singular behavior has been observed for Zn(II) complexes, ZnL, derived from the 1,2-diaminocyclohexane and the 4-methoxysalicylaldehyde. In fact, while in the case of the *cis*-1,2-diaminocyclohexane derivative an asymmetric dimeric aggregate with a typical Zn(II) pentacoordination has been found [7], complexes derived from the enantiopure (1*S*,2*S*)-(+)- or (1*R*,2*R*)-(−)-*trans*-1,2-diaminocyclohexane, **1**, involved the existence of various species in solution [6]. In particular, chloroform solutions of **1** were characterized by the presence of three species, exhibiting a strong concentration dependence, the predominant of which consisting of large oligomeric aggregates. Heating or after standing chloroform solutions of **1** all species are irreversibly converted into a dimer,

1C, which has been described as a dinuclear, double-helicate Zn_2L_2 structure with a tetrahedral coordination around the Zn(II) atoms [6].

The peculiar aggregation features of these chiral complexes are doubtless related to the defined stereochemistry of the *trans*-1,2-diaminocyclohexane bridge. It is, therefore, of interest to further investigate on these complexes, to better understand the physicochemical features responsible for their unusual aggregation behavior. Thus, maintaining the skeleton structure of the chiral ligand we have considered a different substituent on the salicylidene rings, in order to improve the solubility of the related Zn(II) complex in the involved solvents. Accordingly, the complex with the 4-diethylamino substituent, (***R***)-**2**, has been synthesized (Chart 1) with a significant increase of solubility. This, in turn, leads to even more interesting aggregation characteristics in solution which are detailed described in this contribution.

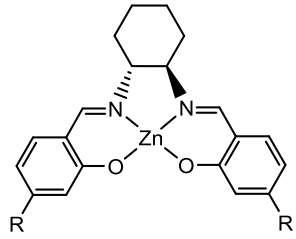

R = OMe; (1*R*,2*R*)- (***R***)-**1**
R = NEt_2; (1*R*,2*R*)- (***R***)-**2**

Chart 1. Investigated Zn(II) Schiff-base complexes.

2. Results

The synthesis of (***R***)-**2** was carried out by standard template method [5–10], using 4-(diethylamino)-2-hydroxybenzaldehyde and (1*R*,2*R*)-*trans*-1,2-diaminocyclohexane in methanol solution and a stoichiometric excess of triethylamine. Then, complexation with the Zn(II) ion was accomplished by using zinc perchlorate. The isolated pale-yellow solid of (***R***)-**2** is very soluble in chloroform and in most polar solvents.

The ^{1}H NMR spectrum of (***R***)-**2** in solution of the coordinating DMSO-d_6 solvent (1.0×10^{-2} M) shows the presence of a single set of signals (Figure 1), independent from the concentration, indicating the existence of monomeric species in solution, as usually observed for Zn(II) Schiff-base complexes [6–11]. To further investigate about the structure of (***R***)-**2** in solution, we performed diffusion-ordered NMR spectroscopy (DOSY) measurements, by using a known internal reference to estimate the molecular mass of species in solution [5–10]. The DOSY spectrum of (***R***)-**2** in DMSO-d_6 (1.0×10^{-2} M) confirms the presence of a single component in the diffusion dimension ($D = 2.5 \times 10^{-10}$ $m^2 \cdot s^{-1}$), with an estimated molecular mass (679 Da) consistent with the (***R***)-**2**·DMSO adduct (Table 1).

The ^{1}H NMR spectrum of (***R***)-**2** in solution of the non-coordinating $CDCl_3$ solvent (1.0×10^{-2} M), unlike the spectrum in DMSO-d_6, appears much more complex for the presence of many signals (Figure 1), indicating the existence of various species in solution. In fact, the related DOSY spectrum is separated into six components, **2A**–**F**, in the diffusion dimension (Figure 2, Table 1), three of them having definitely lower D values ($D \sim 2 \times 10^{-10}$ $m^2 \cdot s^{-1}$) than the remaining three ($D \sim 6 \times 10^{-10}$ $m^2 \cdot s^{-1}$). In particular, assuming **2F** as internal reference dimeric species (vide infra) the molecular mass of remaining components was estimated. Thus, while **2D** and **2E** are also dimeric species, instead **2A**–**C** result to be larger oligomeric aggregates, containing up to 27 monomeric units. In comparison with previous results on the (***R***)-**1** complex in the same non-coordinating chloroform solvent, present data indicate the existence in solution of a greater number of species, some of them having larger estimated molecular masses. This behavior may be related to the greater solubility of (***R***)-**2**, thus allowing for a higher degree of aggregation in solution. Note that, despite the rather

large oligomeric nature of aggregates **2A**–**C**, they are characterized by sharp ^{1}H NMR signals, whose resonance of the imine protons is comparable to that found for the (***R***)-**2**·DMSO adduct (Figure 1). On the other hand, the resonance of the imine protons in **2F** results to be up-field shifted (0.9 ppm) with respect that of **2A**.

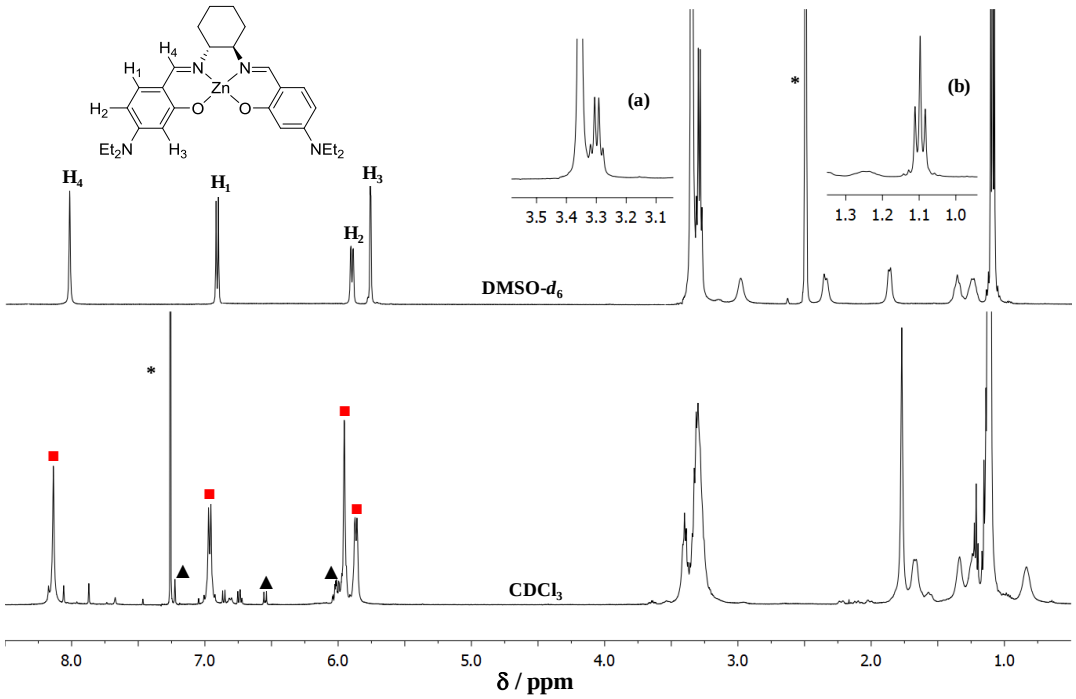

Figure 1. ^{1}H NMR spectra of (***R***)-**2** (1.0×10^{-2} M) in DMSO-d_6 and $CDCl_3$. Asterisks indicate residual solvent peaks. The labeling of the ^{1}H NMR signals related to the $CDCl_3$ solution refers to species (***R***)-**2A** (denoted by the red squares) and (***R***)-**2F** (denoted by the black triangles). Inset: (**a**) expansion of the N-CH_2-CH_3 signal and (**b**) of the N-CH_2-CH_3 signal of (***R***)-**2** in DMSO-d_6.

Table 1. Diffusion coefficients, *D*, and estimated molecular mass, *m*, for (***R***)-**2** in DMSO-d_6 and $CDCl_3$.

Compound	Species	$D \times 10^{10}/m^2 \cdot s^{-1}$	D (solvent) $\times 10^{10}/m^2 \cdot s^{-1}$	m (n) ^{1}/*Da*	m (n) ^{2}/*Da*
(***R***)-**2**	**2**·DMSO-d_6	2.5	7.1(DMSO-d_6)	679 ^{3}	612.2
(***R***)-**2**	**2A**	1.7	26.3($CDCl_3$)	14,046(26.6)	14,256(27)
	2B	1.9	26.3($CDCl_3$)	11,244(21.3)	11,088(21)
	2C	2.2	26.3($CDCl_3$)	8387(15.9)	8448(16)
	2D	5.8	26.3($CDCl_3$)	1207(2.3)	1056(2)
	2E	6.0	26.3($CDCl_3$)	1128(2.1)	1056(2)
	2F	6.2	26.3($CDCl_3$)	1056(2)	1056(2)
(***R***)-**2** ^{4}	**2F**	5.9	24.8 ($CDCl_3$)	1017(1.9)	1056(2)
	1C	6.3	24.8 ($CDCl_3$)	892(2)	891.7(2)

^{1} Estimated molecular mass using the species (***R***)-**2F** as internal reference. Values in parentheses (n) indicate the order of aggregation. ^{2} Expected molecular mass. Values in parentheses (n) indicate the order of aggregation. ^{3} Estimated molecular mass using the solvent as an internal reference. ^{4} $CDCl_3$ solution of (***R***)-**2F** in the presence of (***R***)-**1C** used as internal reference (see Figure S1).

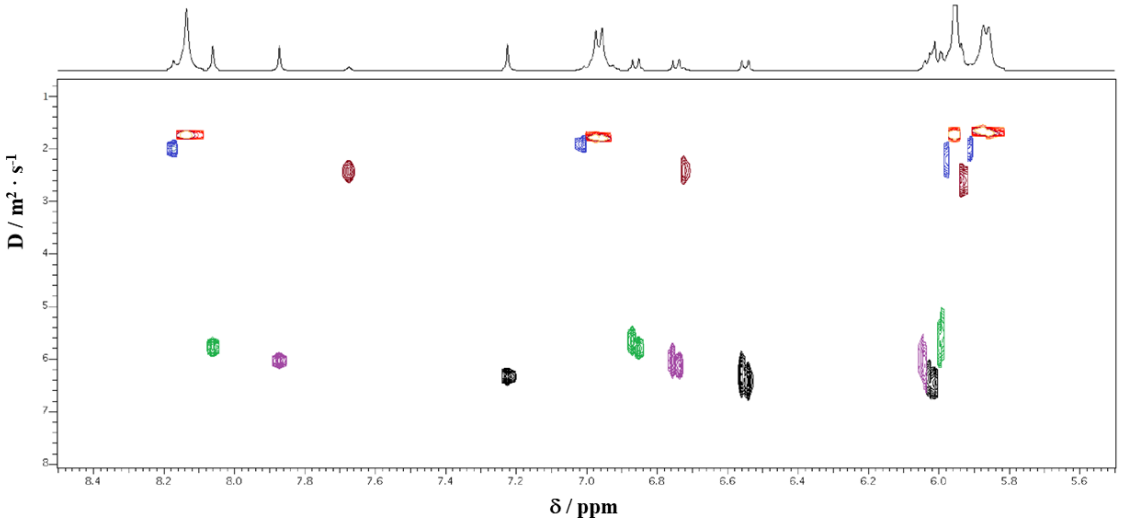

Figure 2. ^{1}H NMR DOSY spectrum of (***R***)-**2** in $CDCl_3$ (1.0×10^{-2} M; 27 °C). Species **2A**–**F** are shown with a different color.

Chloroform solutions of (***R***)-**2** exhibit a pronounced concentration dependence. In particular, starting from concentrated solutions (5.0×10^{-2} M), the progressive dilution leads to a decrease of **2A** and an increase of the other species (Figure S2). In other terms, dilution favors fragmentation of the largest aggregate **2A** into the other oligomers.

Addition of a Lewis base to solutions of non-coordinating solvents of ZnL aggregates generally leads to disaggregation with the formation of monomeric adducts [6–11]. ^{1}H NMR studies of (***R***)-**2** in mixtures of non-coordinating/coordinating ($CDCl_3$/DMSO-d_6) solvents further support the existence of various aggregate species in the former solvent (Figure S3). Actually, the successive addition of defined amounts of DMSO-d_6 (up to ca. 230-fold mole excess) to a freshly prepared $CDCl_3$ solution of (***R***)-**2** leads mainly to the progressive disappearance of oligomer **2A** and the appearance of a new set of signals consistent with the formation of the (***R***)-**2**·DMSO adduct. Only upon addition of ca. 1400-fold mole excess of DMSO-d_6 the complete disappearance of all species is observed, and the resulting solution shows a ^{1}H NMR spectrum almost comparable to that recorded in DMSO-d_6 (Figure 1 and Figure S3). However, even in such large stoichiometric excess the species **2F** remains almost unaltered, indicating a strong stability of this dimeric species.

The relative distribution of aggregates **2A**–**F** exhibits remarkable changes after standing chloroform solutions of (***R***)-**2** at room temperature for some time, as can be evaluated from ^{1}H NMR signals of each species (Figure 3). In particular, freshly prepared chloroform solutions (5.0×10^{-2} M) show the predominant presence of **2A** (82%), while **2B** (6%) and **2C**–**F** (3% each) are minor species. After standing, a progressive conversion of **2A** into **2F** is observed, while the relative percentage of the other species remain almost unchanged. After three weeks, a complete conversion of all species into **2F** is obtained. Moreover, starting from more diluted $CDCl_3$ solutions (5.0×10^{-3} M) the complete conversion of all species into **2F** occurs in a shorter time (one week). An analogous result, that is the complete conversion of all species into **2F**, is achieved by heating chloroform solutions of (***R***)-**2** at 60 °C for four hours.

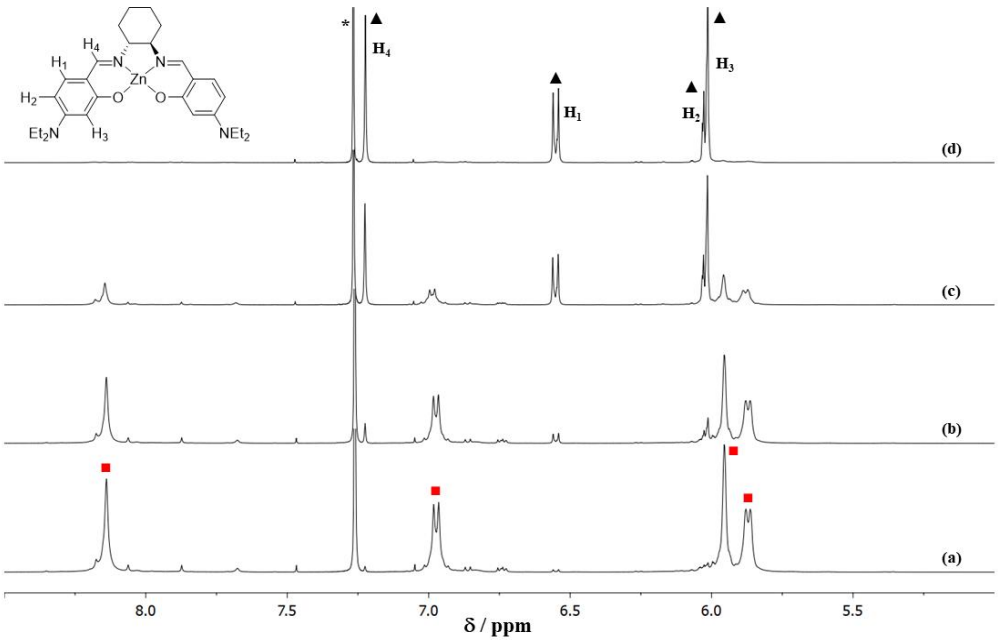

Figure 3. ^{1}H NMR spectra of (***R***)-**2** (5.0×10^{-2} M) in $CDCl_3$ recorded at different time intervals: (**a**) freshly prepared solution; (**b**) after 12 h; (**c**) after one week; and (**d**) after three weeks. The asterisk indicates the residual solvent peak. The labeling of the ^{1}H NMR signals refers to species (***R***)-**2A** (denoted by the red squares) and (***R***)-**2F** (denoted by the black triangles).

The isolated pale-yellow solid obtained from heated $CHCl_3$ solutions of (***R***)-**2** was characterized in chloroform by ESI and DOSY measurements as a dimeric species having identical ^{1}H NMR spectroscopic characteristics of **2F**. Specifically, DOSY experiments were performed using (***R***)-**1C** as an internal reference (Figure S1). The dimeric species **2F** presents some characteristic features previously observed for **1C** [6]. In fact, analogously to **1C**, on passing from DMSO-d_6 solutions of (***R***)-**2** to $CDCl_3$ solutions of **2F** a strong up-field shift, ca. 0.8 ppm, is observed. Moreover, the chemical shift of the C*H*=N signal in **2F** (7.22 ppm) is comparable to that found in **1C** (7.35 ppm).

Optical absorption spectra of (***R***)-**2** in DMSO and $CHCl_3$ solutions are comparable to each other, consisting of a strong band centered at 341 nm and a shoulder at 366 nm (Figure 4), despite the different nature of the involved species in solution: monomeric adduct vs. oligomeric aggregates, respectively. In contrast, the UV–Vis spectrum of (***R***)-**2F** in $CHCl_3$ is very different because, in addition to the absorption band at 341 nm, shows the appearance of a new intense band at longer wavelengths centered at 371 nm, consistent with the existence of strong interligand interactions. These results are indicative of a different aggregation mode on switching from oligomers to the (***R***)-**2F** dimer. On the other hand, no relevant interligand interactions are likely operating in (***R***)-**2** oligomers given the comparable UV–Vis features to those of the monomeric (***R***)-**2**·DMSO adduct.

The differences observed in optical absorption spectra are reflected in circular dichroism (CD) spectra (Figure 4). Thus, while a comparable bisignate signal is observed for solutions of (***R***)-**2** in DMSO and $CHCl_3$, in contrast a stronger and redshifted bisignate signal is noticed for (***R***)-**2F**.

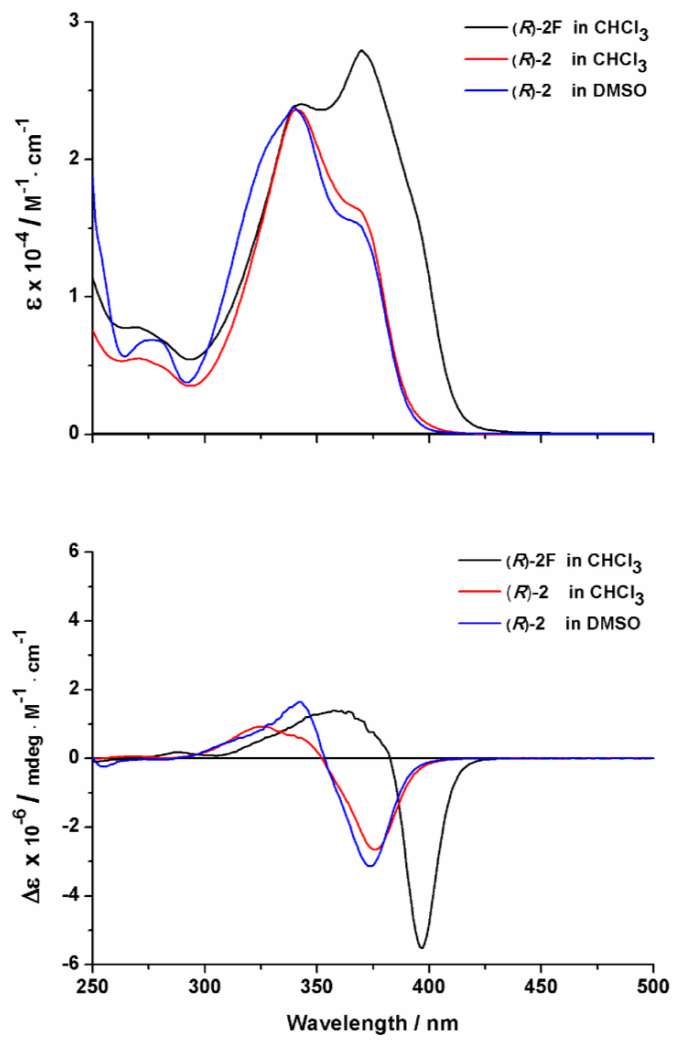

Figure 4. (**Top**) UV–Vis absorption spectra of (***R***)-**2** (5.0×10^{-4} M) in $CHCl_3$ and DMSO, and (***R***)-**2F** (5.0×10^{-4} M) in $CHCl_3$. (**Bottom**) CD spectra of (***R***)-**2** (5.0×10^{-4} M) in $CHCl_3$ and DMSO, and (***R***)-**2F** (5.0×10^{-4} M) in $CHCl_3$.

3. Discussion

For this family of complexes, we have established that the chemical shift of the imine hydrogens is diagnostic of their aggregation mode [5–11]. In particular, the switching from pentacoordinated monomeric adducts in coordinating solvents to dimeric aggregates in chloroform solutions has always accompanied by an up-field shift of these signals, because of the involved hydrogens lie under the shielding zone of the π electrons of a conjugated system [7–11]. Moreover, a further up-field shift has been observed for dinuclear double-helicate structures with a tetrahedral coordination around the Zn(II) metal center, as in **1C**, because of the stronger shielding effects caused by the aromatic ring of the subunit of the other ligand [6]. Relevant chemical shifts for some 4-substituted bis(salicylaldiminato)Zn(II) Schiff-base complexes in $CDCl_3$ solution and their aggregation properties are collected in Table 2. Therefore, given the observed comparable chemical shifts of the C*H*=N signal for **1C** and **2F**, we can hypothesize an analogous dinuclear double-helicate, Zn_2L_2, structure for the latter species. Moreover, **2F** hardly deaggregates with the addition of a Lewis base, such as DMSO. In fact, starting from a 1.0×10^{-2} M $CDCl_3$ solution of **2F** no appreciable variation of ^{1}H NMR signals is observed even after addition of 1.5×10^3-fold mole excess of DMSO-d_6. This indicates a low Lewis acidic character of this dimeric species.

Table 2. Comparison of the C*H*=N chemical shift for some 4-substituted bis(salicylaldiminato)Zn(II) Schiff-base complexes in $CDCl_3$ solution and their aggregation properties.

Diamino Bridge	4-substituent	δ (ppm)	Δδ (ppm) [1]	Zn(II) Coordination	Aggregate Structure	Ref.
2,3-diamino-maleonitrile	$-OC_{11}H_{21}$	8.35	0.03	penta	$(ZnL)_2$	[10]
benzene-1,2-diamine	$-OC_{10}H_{20}$	8.47	0.39	penta	$(ZnL)_2$	[9]
ethane-1,2-diamine	$-OC_{16}H_{33}$	7.61	0.67	penta	$(ZnL)_2$	[8]
cis-cyclohexane-1,2-diamine	–OMe	8.08; 8.33	0.22; −0.03	penta	$(ZnL)_2$	[7]
trans-cyclohexane-1,2-diamine	–OMe	8.33	−0.12	tetra	$(ZnL)_n$ [2]	[6]
		7.35	0.86	tetra	1C, Zn_2L_2	
trans-cyclohexane-1,2-diamine	$-NEt_2$	8.14	−0.11	tetra	2A, $(ZnL)_n$	This work
		7.22	0.81	tetra	2F, Zn_2L_2	
trans-cyclopentane-1,2-diamine	–OMe	7.50	0.69	tetra	Zn_2L_2	[5]

[1] Difference of the chemical shifts between DMSO-d_6 and $CDCl_3$ solutions. [2] Referred to (***R***)-**1** oligomers.

The high degree of aggregation of (***R***)-**2** in freshly-prepared chloroform solutions with the prevalent formation of **2A**, without any broadening of the ^{1}H NMR signals and chemical shifts comparable to those of the monomeric (***R***)-**2**·DMSO adduct, is in contrast to what is commonly observed for other bis(salicylaldiminato)zinc(II) Schiff-base complexes (Table 2). In fact, in the case of intermolecular interactions involving pentacoordinated square-pyramidal Zn(II) geometries, on switching from monomeric adducts to dimeric aggregates, chemical shifts are always up-field shifted, accompanied by a broadening of ^{1}H NMR signals when an oligomerization occurs [7–11]. These observations suggest that in freshly prepared chloroform solutions of (***R***)-**2** a different type aggregation occurs, likely involving a different coordination environment around the metal center, consequence of the preorganized structure of the chiral ligand derived from *trans*-1,2-diaminocyclohexane (Figure 5a). In particular, we hypothesize a tetrahedral coordination geometry in which each metal center is bonded to a bidentate subunit of two different ligands with formation of helical oligomers, $(ZnL)_n$, resulting in no shielding effects on the chemical shift of C*H*=N and aromatic signals. An analogous structure is proposed for (***R***)-**1** oligomers. By standing or heating, chloroform solutions of $(ZnL)_n$ oligomers are irreversibly converted in a more thermodynamically stable, dinuclear double-helicate Zn_2L_2 dimer (**2F** in Figure 5b) having a weak Lewis acidic character.

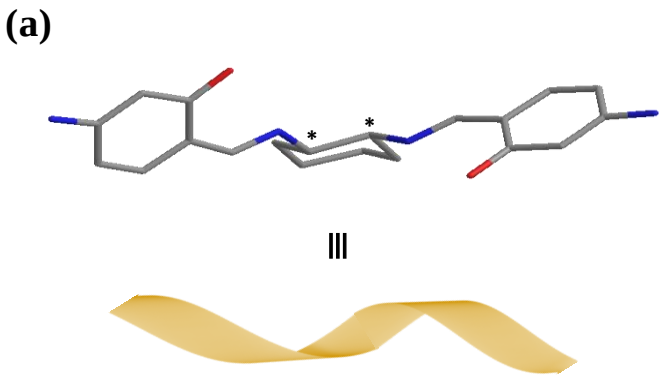

Figure 5. *Cont.*

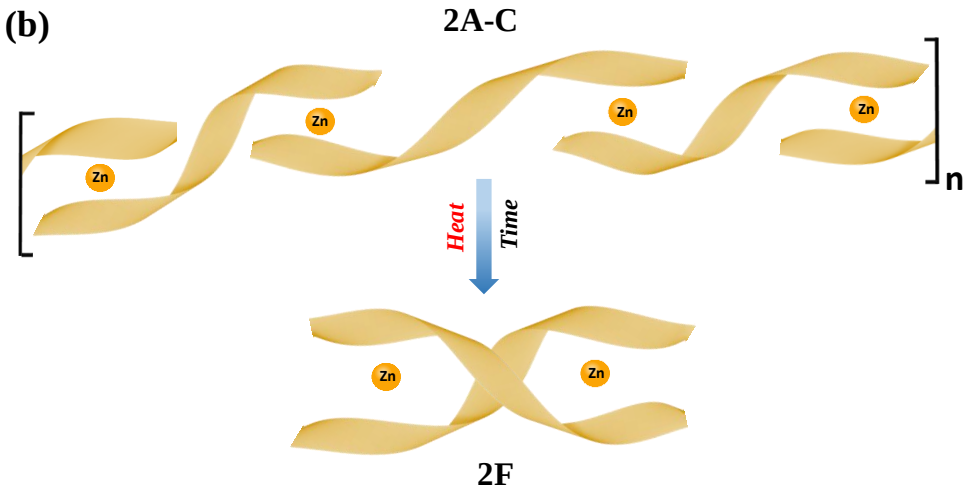

Figure 5. (**a**) DFT optimized geometry (B3LYP) for the chiral ligand derived from *trans*-1,2-diaminocyclohexane. Hydrogens and ethyl groups are omitted for clarity. (**b**) Proposed helical structure for oligomeric aggregates of (***R***)-**2** in chloroform solution. By heating, or after standing, oligomers are irreversibly converted into a thermodynamically stable, dinuclear double-helicate dimer **2F**. Both the oligomers and the dimer involve a tetrahedral coordination geometry around the metal center.

This picture is fully consistent with the optical absorption and circular dichroism spectroscopic results. In fact, $(ZnL)_n$ oligomers behave as monomeric (***R***)-**2**·DMSO adducts, with no evidence of relevant interactions between the subunits of two different ligands, since no shift of the UV–Vis spectral feature, related to $\pi \rightarrow \pi^*$ transitions [54], is observed. In contrast, these interactions are operating in the double-helicate Zn_2L_2 dimer with consequent red-shift and hyperchromism of the longer wavelength absorption band. Due to the chiral *trans*-1,2-diaminocyclohexane bridge all involved species exhibit a bisignate CD signal characteristic of helical structures.

4. Experimental Section

4.1. Materials and General Procedures

All the reactions were executed under nitrogen. Zinc perchlorate hexahydrate, 4-(diethylamino)-2-hydroxybenzaldehyde, (1*R*,2*R*)-1,2-diaminocyclohexane, and triethylamine (Aldrich, Milan, Italy) were used as received. Chloroform (Aldrich, Milan, Italy) stabilized with amylene was used for UV–Vis and CD measurements. $CDCl_3$ (Aldrich, Milan, Italy) was stored over molecular sieves (3 Å), while DMSO-d_6 was used as obtained.

4.2. Physical Measurements

Elemental analyses were performed on a Carlo Erba 1106 elemental analyzer (Carlo Erba, Milan, Italy). ESI-MS spectra were recorded on a AB Sciex API 2000 LC/MS/MS System (AB Sciex Italia, Milan, Italy). All NMR experiments were recorded at 27 °C on a Varian Unity S 500 spectrometer (Varian, Palo Alto, CA, USA), using tetramethylsilane ($Si(CH_3)_4$, TMS) as an internal reference. DOSY experiments were performed as reported elsewhere [5–10]. Optical absorption and CD spectra were recorded at room temperature using a UV–Vis Jasco V-630 spectrophotometer (Jasco Europe, Cremella (LC), Italy) and a Jasco 810 spectropolarimeter (Jasco Europe, Cremella (LC), Italy), respectively. All UV–Vis and CD measurements were recorded using a 1 mm path length cuvette.

4.3. Computational Method

Geometry optimization for the ligand was performed by means of first principle DFT calculations, using Becke's three-parameter exchange functional supplemented with the Lee-Yang-Parr correlation functional, B3LYP [55,56]. The tight optimization criteria along with an ultrafine grid were adopted for the geometry optimization. Calculations were computed with the Gaussian 09 program [57] using the 6-31G basis set.

4.4. Syntheses

4.4.1. {*N*,*N*-Bis[4-(diethylamino)-2-hydroxybenzylidene]-(1*R*,2*R*)-trans-1,2-diaminocyclohexane-diaminato}Zn(II) (***R***)-**2**

(1*R*,2*R*)-1,2-Diaminocyclohexane (0.114 g, 1.00 mmol) was dissolved in methanol (20.0 mL). Then, 4-(diethylamino)-2-hydroxybenzaldehyde (0.387 g, 2.00 mmol) was added. The mixture obtained was heated at reflux with stirring for 2 h. The yellow solution so obtained was treated with zinc perchlorate hexahydrate (0.372 g, 1.00 mmol) and triethylamine (1.00 mL) to obtain a mixture that was refluxed and stirred overnight. After cooling to room temperature, the precipitated solid was collected by filtration, washed with methanol, and dried in a vacuum desiccator at 120 °C over sulfuric acid. Pale-yellow powder (0.502 g, 95%). $C_{28}H_{38}N_4O_2Zn$ (528.02): Calcd. C, 63.69; H, 7.25; N, 10.61; Found C, 63.58; H, 7.24; N, 10.63. ^{1}H NMR (500 MHz, DMSO-d_6): δ = 1.10 (t, $^3J_{HH}$ = 7.0 Hz, 12H, NCH_2CH_3), 1.24 (br, 2H, cyclohexyl-*H*), 1.36 (br, 2H, cyclohexyl-*H*), 1.87 (br, 2H, cyclohexyl-*H*), 2.35 (br, 2H, cyclohexyl-H), 2.99 (br, 2H, CH–N=CH), 3.30 (q, $^3J_{HH}$ = 7.0 Hz, 8H; NCH_2CH_3), 5.77 (d, $^4J_{HH}$ = 2.0 Hz, 2H; ArH), 5.91 (dd, $^3J_{HH}$ = 8.5 Hz, $^4J_{HH}$ = 2.0 Hz, 2H; ArH), 6.91 (d, $^3J_{HH}$ = 8.5 Hz, 2H; ArH), 8.02 (s, 2H; CH=N). ^{13}C NMR (125 MHz, DMSO-d_6): δ = 12.86, 24.10, 27.80, 43.67, 64.30, 99.30, 101.86, 110.58, 136.51, 151.25, 161.82, 163.02.

4.4.2. (***R***)-**2F**

A sample of (***R***)-**2** (0.0528 g, 0.10 mmol) was dissolved in chloroform (10 mL) and refluxed under nitrogen until all the other species **2A**–**E** disappeared in the ^{1}H NMR spectrum (typically four hours). The solvent was evaporated under vacuum to give **2F** as pale-yellow powder in quantitative yield. ESI-MS: m/z = 1053 $[M + H]^+$, 1075 $[M + Na]^+$. ^{1}H NMR (500 MHz, $CDCl_3$): δ = 1.21 (t, $^3J_{HH}$ = 7.0 Hz, 24H; NCH_2CH_3), 1.25 (br, 4H, cyclohexyl-H), 1.56 (br, 4H, cyclohexyl-H), 1.65 (br, 8H, cyclohexyl-H), 3.31 (br, 4H, –CH–N=CH), 3.39 (q, $^3J_{HH}$ = 7.0 Hz, 16H; NCH_2CH_3), 6.02 (m, 8H; ArH), 6.55 (d, $^3J_{HH}$ = 10.0 Hz, 4H; ArH), 7.22 (s, 4H; CH=N). ^{13}C NMR (125 MHz, $CDCl_3$): δ = 12.95, 25.29, 37.87, 44.46, 68.61, 101.03, 101.43, 109.97, 138.37, 153.18, 169.23, 171.55.

5. Conclusions

This study further demonstrated the intriguing and variegate aggregation characteristics of bis(salicylaldiminato)zinc(II) Schiff-base complexes. Thanks to the 4-diethylamino substituent on the salicylidene rings, the greater solubility of (***R***)-**2**, in comparison with the (***R***)-**1** analogue, allows a higher degree of aggregation in solution. The chiral *trans*-stereochemistry of the bridging diamine favors a different aggregation mode in these complexes, either in the oligomers and dimers, involving a tetrahedral coordination geometry around the metal center. Experimental data suggest the formation of helical oligomers, $(ZnL)_n$, in freshly-prepared solutions of non-coordinating solvents which, by standing or heating, evolve towards a more thermodynamically stable, dinuclear double-helicate Zn_2L_2 dimer.

Supplementary Materials: The following are available online at www.mdpi.com/2304-6740/6/1/8/s1. Figure S1: ^{1}H NMR DOSY spectrum of (***R***)-**2F** in the presence of (***R***)-**1C** used as internal reference; Figure S2: Concentration dependence of ^{1}H NMR spectra of (***R***)-**2** in $CDCl_3$ solution; Figure S3: ^{1}H NMR spectra of (***R***)-**2** in $CDCl_3$ (1.0×10^{-2} M; 6.0×10^{-6} mol) (**a**), and with addition of 2.8×10^{-4} mol (**b**), 7.0×10^{-4} mol (**c**), 1.4×10^{-3} mol (**d**), and 8.4×10^{-3} mol (**e**) of DMSO-d_6.

Acknowledgments: This research was supported by the MIUR and the University of Catania.

Author Contributions: Giuseppe Consiglio and Ivan Pietro Oliveri performed the experiments. Salvatore Failla and Santo Di Bella conceived the project and supervised the work. All authors discussed the results, interpreted the data, and contributed to the preparation of the final manuscript.

Conflicts of Interest: The authors declare no conflict of interest.

References

1. Steed, J.W.; Atwood, J.L. *Supramolecular Chemistry*, 2rd ed.; Wiley: Hoboken, NJ, USA, 2009; ISBN 978-0-470-51233-3.
2. Babu, S.S.; Praveen, V.K.; Ajayaghosh, A. Functional π-gelators and their applications. *Chem. Rev.* **2014**, *114*, 1973–2129. [CrossRef] [PubMed]
3. Wong, K.M.-C.; Yam, W.-W. Self-assembly of luminescent alkynylplatinum(II) terpyridyl complexes: Modulation of photophysical properties through aggregation behavior. *Acc. Chem. Res.* **2011**, *44*, 424–434. [CrossRef] [PubMed]
4. Hong, Y.; Lam, J.W.Y.; Tang, B.Z. Aggregation-induced emission. *Chem. Soc. Rev.* **2011**, *40*, 5361–5388. [CrossRef] [PubMed]
5. Oliveri, I.P.; Forte, G.; Consiglio, G.; Failla, S.; Di Bella, S. Aggregates of defined stereochemical scaffolds: A study in solution of a zinc(II) Schiff base complex derived from the enantiopure *trans*-1,2-cyclopentanediamine. *Inorg. Chem.* **2017**, *56*, 14206–14213. [CrossRef] [PubMed]
6. Consiglio, G.; Oliveri, I.P.; Failla, S.; Di Bella, S. Supramolecular aggregates of defined stereochemical scaffolds: Aggregation/deaggregation in Schiff-base zinc(II) complexes derived from enantiopure *trans*-1,2-diaminocyclohexane. *Inorg. Chem.* **2016**, *55*, 10320–10328. [CrossRef] [PubMed]
7. Consiglio, G.; Oliveri, I.P.; Punzo, F.; Thompson, A.L.; Di Bella, S.; Failla, S. Structure and aggregation properties of a Schiff-base zinc(II) complex derived from *cis*-1,2-diaminocyclohexane. *Dalton Trans.* **2015**, *44*, 13040–13048. [CrossRef] [PubMed]
8. Consiglio, G.; Failla, S.; Finocchiaro, P.; Oliveri, I.P.; Di Bella, S. An unprecedented structural interconversion in solution of aggregate zinc(II) salen Schiff-base complexes. *Inorg. Chem.* **2012**, *51*, 8409–8418. [CrossRef] [PubMed]
9. Consiglio, G.; Failla, S.; Finocchiaro, P.; Oliveri, I.P.; Di Bella, S. Aggregation properties of bis(salicylaldiminato)zinc(II) Schiff-base complexes and their Lewis acidic character. *Dalton Trans.* **2012**, *41*, 387–395. [CrossRef] [PubMed]
10. Consiglio, G.; Failla, S.; Finocchiaro, P.; Oliveri, I.P.; Purrello, R.; Di Bella, S. Supramolecular aggregation/deaggregation in amphiphilic dipolar Schiff-base zinc(II) complexes. *Inorg. Chem.* **2010**, *49*, 5134–5142. [CrossRef] [PubMed]
11. Consiglio, G.; Failla, S.; Oliveri, I.P.; Purrello, R.; Di Bella, S. Controlling the molecular aggregation. An amphiphilic Schiff-base zinc(II) complex as supramolecular fluorescent probe. *Dalton Trans.* **2009**, 10426–10428. [CrossRef] [PubMed]
12. Forte, G.; Oliveri, I.P.; Consiglio, G.; Failla, S.; Di Bella, S. On the Lewis acidic character of bis(salicylaldiminato)zinc(II) Schiff-base complexes: A computational and experimental investigation on a series of compounds varying the bridging diimine. *Dalton Trans.* **2017**, *46*, 4571–4581. [CrossRef] [PubMed]
13. Groizard, T.; Kahlal, S.; Dorcet, V.; Roisnel, T.; Bruneau, C.; Halet, J.-F.; Gramage-Doria, R. Nonconventional supramolecular self-assemblies of zinc(II)-salphen building blocks. *Eur. J. Inorg. Chem.* **2016**, 5143–5151. [CrossRef]
14. Oliveri, I. P.; Failla, S.; Colombo, A.; Dragonetti, C.; Righetto, S.; Di Bella, S. Synthesis, characterization, optical absorption/fluorescence spectroscopy, and second-order nonlinear optical properties of aggregate molecular architectures of unsymmetrical Schiff-base zinc(II) complexes. *Dalton Trans.* **2014**, *43*, 2168–2175. [CrossRef] [PubMed]
15. Oliveri, I.P.; Failla, S.; Malandrino, G.; Di Bella, S. New molecular architectures by aggregation of tailored zinc(II) Schiff-base complexes. *New J. Chem.* **2011**, *35*, 2826–2831. [CrossRef]
16. Wezenberg, S.J.; Escudero-Adán, E.C.; Benet-Buchholz, J.; Kleij, A.W. Anion-templated formation of supramolecular multinuclear assemblies. *Chem. Eur. J.* **2009**, *15*, 5695–5700. [CrossRef] [PubMed]

17. Gallant, A.J.; Chong, J.H.; MacLachlan, M.J. Heptametallic bowl-shaped complexes derived from conjugated Schiff-base macrocycles: Synthesis, characterization, and X-ray crystal structures. *Inorg. Chem.* **2006**, *45*, 5248–5250. [CrossRef] [PubMed]
18. Kleij, A.W.; Kuil, M.; Tooke, D.M.; Lutz, M.; Spek, A.L.; Reek, J.N.H. Zn^{II}-salphen complexes as versatile building blocks for the construction of supramolecular box assemblies. *Chem. Eur. J.* **2005**, *11*, 4743–4750. [CrossRef] [PubMed]
19. Chakraborty, S.; Mondal, P.; Prasad, S.K.; Rao, D.S.S.; Bhattacharjee, C.R. Zinc(II)-salphen complexes bearing long alkoxy side arms: Synthesis, solvent dependent aggregation, and spacer group substituent effect on mesomorphism and photophysical property. *J. Mol. Liq.* **2017**, *246*, 290–301. [CrossRef]
20. Chakraborty, S.; Mondal, P.; Prasad, S.K.; Rao, D.S.S.; Bhattacharjee, C.R. Induction of mesomorphism through supramolecular assembly in metal coordination compounds of "salphen"-type Schiff Bases: Photoluminescence and solvatochromism. *Eur. J. Inorg. Chem.* **2016**, 4604–4614. [CrossRef]
21. Chakraborty, S.; Bhattacharjee, C.R.; Mondal, P.; Prasad, S.K.; Rao, D.S.S. Synthesis and aggregation behaviour of luminescent mesomorphic zinc(II) complexes with 'salen' type asymmetric Schiff base ligands. *Dalton Trans.* **2015**, *44*, 7477–7488. [CrossRef] [PubMed]
22. Pucci, D.; Aiello, I.; Bellusci, A.; Crispini, A.; Ghedini, M.; La Deda, M. Coordination induction of nonlinear molecular shape in mesomorphic and luminescent Zn^{II} complexes based on salen-like frameworks. *Eur. J. Inorg. Chem.* **2009**, 4274–4281. [CrossRef]
23. Piccinno, M.; Angulo-Pachón, C.A.; Ballester, P.; Escuder, B.; Dalla Cort, A. Rational design of a supramolecular gel based on a Zn(II)-salophen bis-dipeptide derivative. *RSC Adv.* **2016**, *6*, 57306–57309. [CrossRef]
24. Oliveri, I.P.; Malandrino, G.; Di Bella, S. Self-assembled nanostructures of amphiphilic Zinc(II) salophen complexes: Role of the solvent on their structure and morphology. *Dalton Trans.* **2014**, *43*, 10208–10214. [CrossRef] [PubMed]
25. Oliveri, I.P.; Failla, S.; Malandrino, G.; Di Bella, S. Controlling the molecular self-assembly into nanofibers of amphiphilic zinc(II) salophen complexes. *J. Phys. Chem. C* **2013**, *117*, 15335–15341. [CrossRef]
26. Hui, J. K.-H.; MacLachlan, M. J. Fibrous aggregates from dinuclear zinc(II) salphen complexes. *Dalton Trans.* **2010**, *39*, 7310–7319. [CrossRef] [PubMed]
27. Hui, J.K.-H.; Yu, Z.; MacLachlan, M.J. Supramolecular assembly of zinc salphen complexes: Access to metal-containing gels and nanofibers. *Angew. Chem. Int. Ed.* **2007**, *46*, 7980–7983. [CrossRef] [PubMed]
28. Wang, W.-J.; Hao, L.; Chen, C.-Y.; Qiu, Q.-M.; Wang, K.; Song, J.-B.; Li, H. Red-shift in fluorescence emission of D-A type asymmetrical Zn(II) complexes by extending the π–π stacking interaction. *RSC Adv.* **2017**, *7*, 20488–20493. [CrossRef]
29. Minei, P.; Fanizza, E.; Rodríguez, A.M.; Muñoz-García, A.B.; Cimino, P.; Pavone, M.; Pucci, A. Cost-effective solar concentrators based on red fluorescent Zn(II)-salicylaldiminato complex. *RSC Adv.* **2016**, *6*, 17474–17482. [CrossRef]
30. Dumur, F.; Contal, E.; Wantz, G.; Gigmes, D. Photoluminescence of zinc complexes: Easily tunable optical properties by variation of the bridge between the imido groups of Schiff base ligands. *Eur. J. Inorg. Chem.* **2014**, 4186–4198. [CrossRef]
31. Di Bella, S.; Oliveri, I.P.; Colombo, A.; Dragonetti, C.; Righetto, S.; Roberto, D. An unprecedented switching of the second-order nonlinear optical response in aggregate bis(salicylaldiminato)zinc(II) Schiff-base complexes. *Dalton Trans.* **2012**, *41*, 7013–7016. [CrossRef] [PubMed]
32. Dalla Cort, A.; De Bernardin, P.; Forte, G.; Mihan, F.Y. Metal-salophen-based receptors for anions. *Chem. Soc. Rev.* **2010**, *39*, 3863–3874. [CrossRef] [PubMed]
33. Yin, H.-Y.; Tang, J.; Zhang, J.-L. Introducing metallosalens to biological studies: The renaissance of traditional coordination complexes. *Eur. J. Inorg. Chem.* **2017**, 5085–5093. [CrossRef]
34. Oliveri, I.P.; Di Bella, S. Lewis basicity of relevant monoanions in a non-protogenic organic solvent using a zinc(II) Schiff-base complex as reference Lewis acid. *Dalton Trans.* **2017**, *46*, 11608–11614. [CrossRef] [PubMed]
35. Mirabella, S.; Oliveri, I.P.; Ruffino, F.; Maccarrone, G.; Di Bella, S. Low-cost chemiresistive sensor for volatile amines based on a 2D network of a zinc(II) Schiff-base complex. *Appl. Phys. Lett.* **2016**, *109*, 143108. [CrossRef]

36. Cheng, J.; Gou, F.; Zhang, X.; Shen, G.; Zhou, X.; Xiang, H. A class of multiresponsive colorimetric and fluorescent pH probes via three different reaction mechanisms of salen complexes: A Selective and Accurate pH Measurement. *Inorg. Chem.* **2016**, *55*, 9221–9229. [CrossRef] [PubMed]
37. Martínez-Rodríguez, L.; Bandeira, N.A.G.; Bo, C.; Kleij, A.W. Highly efficient chirality transfer from diamines encapsulated within a self-assembled calixarene-salen host. *Chem. Eur. J.* **2015**, *21*, 7144–7150. [CrossRef] [PubMed]
38. Sabaté, F.; Giannicchi, I.; Acóna, L.; Dalla Cort, A.; Rodríguez, L. Anion selectivity of Zn-salophen receptors: Influence of ligand substituents. *Inorg. Chim. Acta* **2015**, *434*, 1–6. [CrossRef]
39. Kumari, N.; Zelder, F. Detecting biologically relevant phosphates with locked salicylaldehyde probes in water. *Chem. Commun.* **2015**, *51*, 17170–17173. [CrossRef] [PubMed]
40. Tang, J.; Cai, Y.-B.; Jing, J.; Zhang, J.-L. Unravelling the correlation between metal induced aggregation and cellular uptake/subcellular localization of znsalen: an overlooked rule for design of luminescent metal probes. *Chem. Sci.* **2015**, *6*, 2389–2397. [CrossRef] [PubMed]
41. Oliveri, I.P.; Malandrino, G.; Di Bella, S. Phase transition and vapochromism in molecular assemblies of a polymorphic zinc(II) Schiff-base complex. *Inorg. Chem.* **2014**, *53*, 9771–9777. [CrossRef] [PubMed]
42. Cheng, J.; Ma, X.; Zhang, Y.; Liu, J.; Zhou, X.; Xiang, H. Optical chemosensors based on transmetalation of salen-based Schiff base complexes. *Inorg. Chem.* **2014**, *53*, 3210–3219. [CrossRef] [PubMed]
43. Brissos, R.; Ramos, D.; Lima, J.C.; Yafteh Mihan, F.; Borràs, M.; de Lapuente, J.; Dalla Cort, A.; Rodríguez, L. Luminescent zinc salophen derivatives: Cytotoxicity assessment and action mechanism studies. *New J. Chem.* **2013**, *37*, 1046–1055. [CrossRef]
44. Jurček, O.; Cametti, M.; Pontini, M.; Kolehmainena, E.; Rissanen, K. A Zinc-salophen/bile-acid conjugate receptor solubilized by CTABr micelles binds phosphate in water. *Org. Biomol. Chem.* **2013**, *11*, 4585–4590. [CrossRef] [PubMed]
45. Strianese, M.; Milione, S.; Maranzana, A.; Grassi, A.; Pellecchia, C. Selective detection of ATP and ADP in aqueous solution by using a fluorescent zinc receptor. *Chem. Commun.* **2012**, *48*, 11419–11421. [CrossRef] [PubMed]
46. Yafteh Mihan, F.; Bartocci, S.; Bruschini, M.; De Bernardin, P.; Forte, G.; Giannicchi, I.; Dalla Cort, A. Ion-pair recognition by metal-salophen and metal-salen complexes. *Aust. J. Chem.* **2012**, *65*, 1638–1646. [CrossRef]
47. Oliveri, I.P.; Maccarrone, G.; Di Bella, S. A Lewis basicity scale in dichloromethane for amines and Common nonprotogenic solvents using a zinc(II) Schiff-base complex as reference Lewis acid. *J. Org. Chem.* **2011**, *76*, 8879–8884. [CrossRef] [PubMed]
48. Oliveri, I.P.; Di Bella, S. Sensitive fluorescent detection and Lewis basicity of aliphatic amines. *J. Phys. Chem. A* **2011**, *115*, 14325–14330. [CrossRef] [PubMed]
49. Oliveri, I.P.; Di Bella, S. Highly sensitive fluorescent probe for detection of alkaloids. *Tetrahedron* **2011**, *67*, 9446–9449. [CrossRef]
50. Khatua, S.; Choi, S.H.; Lee, J.; Kim, K.; Do, Y.; Churchill, D.G. Aqueous fluorometric and colorimetric sensing of phosphate ions by a fluorescent dinuclear zinc complex. *Inorg. Chem.* **2009**, *48*, 2993–2999. [CrossRef] [PubMed]
51. Cano, M.; Rodríguez, L.; Lima, J.C.; Pina, F.; Dalla Cort, A.; Pasquini, C.; Schiaffino, L. Specific supramolecular interactions between Zn^{2+}-salophen complexes and biologically relevant anions. *Inorg. Chem.* **2009**, *48*, 6229–6235. [CrossRef] [PubMed]
52. Dalla Cort, A.; Bernardin, P.; Schiaffino, L. A new water soluble Zn-salophen derivative as a receptor for α-aminoacids: Unexpected chiral DISCRIMINATION. *Chirality* **2009**, *21*, 104–109. [CrossRef] [PubMed]
53. Escudero-Adán, E.C.; Benet-Buchholz, J.; Kleij, A.W. Supramolecular adsorption of alkaloids by metallosalphen complexes. *Inorg. Chem.* **2008**, *47*, 4256–4263. [CrossRef] [PubMed]
54. Vladimirova, K.G.; Freidzon, A.Y.; Kotova, O.V.; Vaschenko, A.A.; Lepnev, L.S.; Bagatur'yants, A.A.; Vitukhnovskiy, A.G.; Stepanov, N.F.; Alfimov, M.V. Theoretical study of structure and electronic absorption spectra of some Schiff bases and their zinc complexes. *Inorg. Chem.* **2009**, *48*, 11123–11130. [CrossRef] [PubMed]
55. Becke, A.D. Density-functional exchange-energy approximation with correct asymptotic behavior. *Phys. Rev. A* **1988**, *38*, 3098–3100. [CrossRef]
56. Lee, C.; Yang, W.; Parr, R.G. Development of the Colle-Salvetti correlation-energy formula into a functional of the electron density. *Phys. Rev. B* **1988**, *37*, 785–789. [CrossRef]

57. Frisch, M.J.; Trucks, G.W.; Schlegel, H.B.; Scuseria, G.E.; Robb, M.A.; Cheeseman, J.R.; Scalmani, G.; Barone, V.; Mennucci, B.; Petersson, G.A.; et al. Gaussian 09, revision A.02. Gaussian, Inc.: Wallingford, CT, USA, 2009.